Thermochemistry of paddle wheel MOFs: Cu-HKUST-1 and Zn-HKUST-1

ARTICLE *in* LANGMUIR · MAY 2013

Impact Factor: 4.46 · DOI: 10.1021/la4012839 · Source: PubMed

Langmuir

Article

pubs.acs.org/Langmuir

Thermochemistry of Paddle Wheel MOFs: Cu-HKUST-1 and Zn-HKUST-1

Manas K. Bhunia,[†] James T. Hughes,[†] James C. Fettinger,[‡] and Alexandra Navrotsky*,[†]

[†]Peter A. Rock Thermochemistry Laboratory and NEAT ORU, University of California, Davis, One Shields Ave., Davis, California 95616, United States

[‡]Department of Chemistry, University of California, Davis, One Shields Ave., Davis, California 95616, United States

Supporting Information

ABSTRACT: Metal−organic framework (MOF) porosity relies upon robust metal−organic bonds to retain structural rigidity upon solvent removal. Both the as-synthesized and activated Cu and Zn polymorphs of HKUST-1 were studied by room temperature acid solution calorimetry. Their enthalpies of formation from dense assemblages (metal oxide (ZnO or CuO), trimesic acid (TMA), and *N*,*N*-dimethylformamide (DMF)) were calculated from the calorimetric data. The enthalpy of formation (ΔH_f) of the as-synthesized Cu-HKUST-H_2O ($[Cu_3TMA_2{\cdot}3H_2O]{\cdot}5DMF$) is −52.70 ± 0.34 kJ per mole of Cu. The ΔH_f for Zn-HKUST-DMF ($[Zn_3TMA_2{\cdot}3DMF]{\cdot}2DMF$) is −54.22 ± 0.57 kJ per mole of Zn. The desolvated Cu-HKUST-dg [Cu_3TMA_2] has a ΔH_f of 16.66 ± 0.51 kJ/mol per mole Cu. The ΔH_f for Zn-HKUST-amorph [$Zn_3TMA_2{\cdot}2DMF$] is −3.57 ± 0.21 kJ per mole of Zn. Solvent stabilizes the Cu-HKUST-H_2O by −69.4 kJ per mole of Cu and Zn-HKUST-DMF by at least −50.7 kJ per mole of Zn. Such strong chemisorption of solvent is similar in magnitude to the strongly exothermic binding at low coverage for chemisorbed H_2O on transition metal oxide nanoparticle surfaces. The strongly exothermic solvent−framework interaction suggests that solvent can play a critical role in obtaining a specific secondary building unit (SBU) topology.

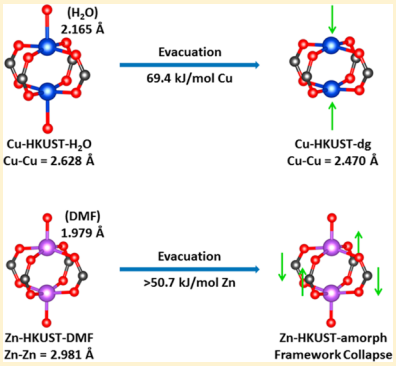

INTRODUCTION

Metal−organic frameworks (MOFs) are a unique class of porous hybrid materials. They combine metal secondary building units (SBU) with multidentate organic linking molecules, which together form porous crystalline motifs. The hybrid nature of MOFs provides a high level of synthetic control, making them well suited for customization for specific applications.[1−10] Yet identifying which MOFs are stable or persistent and which have the desired functionality is still largely an empirical process.[11] Solvent is one of several critical parameters (others being temperature, pressure, concentration, etc.) from which to choose in synthesis optimization. In previous thermochemical studies of porous inorganic materials[12,13] and of other MOFs,[14,15] solvent was seen as filling space. The enthalpy of solvent−framework interaction is weak (1.0−6.0 kJ per mol tetrahedra) and does not actively stabilize the structure. In MOF-5, *N*,*N*-diethylformamide (DEF) was shown to stabilize by only −4.8 kJ per mole of Zn.[14] Similarly, *N*,*N*-dimethylformamide (DMF) stabilizes ZIF-4 by only −3.0 kJ per mole of Zn.[15] However, both these frameworks have secondary building units (SBUs) which do not contain open solvent binding sites. In contrast, the paddle wheel SBUs studied in this report are constructed from four carboxylate groups which bind two metal atoms together. The carboxylate group syn−syn bonding confines the two metal centers along a central rotation axis, giving the SBU D_{4h} symmetry (Figure 1). The unobstructed axial face of each metal center is free to chemisorb one solvent molecule, giving a total of two binding

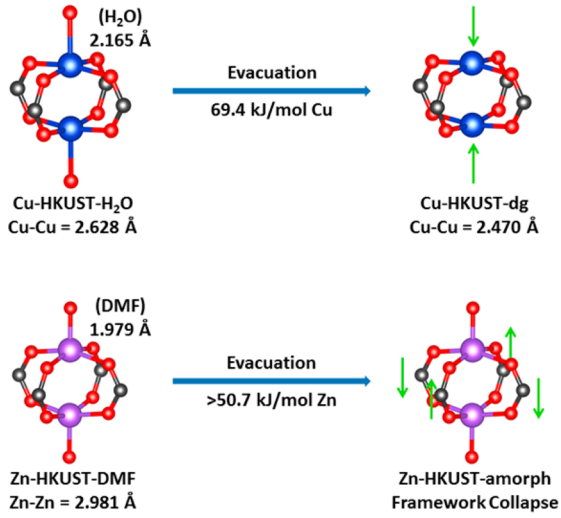

Figure 1. Coordination environment around the Cu and Zn paddle wheel SBU in the HKUST structure and the energetic increase per mole of SBU upon solvent removal.[45] Zn-HKUST-DMF becomes unstable upon removal of the first DMF molecule, collapsing into an amorphous structure. Trimesic acid is omitted for clarity.

Received: April 8, 2013
Revised: May 30, 2013
Published: May 31, 2013

   dx.doi.org/10.1021/la4012839 | *Langmuir* 2013, 29, 8140−8145

Table 1. Chemical Properties of HKUST-1 (Cu and Zn)

compound	molecular formula	no. solvent coordinated	molecules uncoordinated	framework density[a] M/nm^3
Cu-HKUST-H_2O	$[Cu_3(TMA)_2{\cdot}3H_2O]{\cdot}5DMF$	3 (H_2O)	5 (DMF)	2.63
Cu-HKUST-dg	$[Cu_3(TMA)_2]$			2.63
Zn-HKUST-DMF	$[Zn_3TMA_2{\cdot}3DMF]{\cdot}2DMF$	3 (DMF)	2 (DMF)	2.57
Zn-HKUST-amorph	$[Zn_3TMA_2{\cdot}2DMF]$	2 (DMF)		

[a]Framework density is determined from the crystal structures of Cu-HKUST-H_2O and Zn-HKUST-DMF.

sites per SBU. Metal carboxylate paddle wheel SBUs are quite common and are found in a multitude of hybrid material structures ranging from 0-D to 3-D frameworks.[16]

Structural variation in the paddle-wheel clusters largely depends on changes in the size geometry of the coordination sphere of the metal atom. Thus, minor variations in the coordination chemistry can have profound effects on the structure and stability of a paddle wheel SBU and, in turn, on the entire MOF. It has recently been shown that the isostructural MOFs with Cu-based paddle wheel SBUs appear to be more stable than their Zn-analogues.[17]

Zinc paddle wheel SBUs can show dynamic structural transformations upon the removal and rebinding of guest molecules.[18] Kitagawa et al. described this feature as "soft porosity" which originates from the stereochemical environment around the SBU.[19] An underlying question is whether the differences in the persistence versus collapse of various MOFs are due to thermodynamic factors (differences in free energy of the open versus collapsed structure), kinetic factors (different rates and activation energies for structural collapse) or a combination of both.

HKUST-1 is one of the first reported MOFs,[20] employing Cu based paddle wheel SBU which are linked together by trimesic acid (TMA) linkers (Figure 1). Others have synthesized the HKUST-1 framework with several different metal atoms: Cu, Zn, Co, and Ni.[21,22] The Cu version notably displays persistence in both water and air, and is marketed by BASF as BASOLITE C300.[20] In contrast, the Zn paddle-wheel MOFs collapse upon removal of guest molecules.[22] The chemical sensitivity of the Zn framework is not uncommon for zinc carboxylate MOFs,[23] yet the paddle wheel zinc carboxylates exhibit an additional degree of instability.[18] This study examines the thermochemistry of the Cu and Zn polymorphs of the HKUST-1 framework to address whether this difference in apparent stability is primarily the result of thermodynamic driving forces or kinetic factors. The as-synthesized (Cu-HKUST-H_2O and Zn-HKUST-DMF) and degassed (Cu-HKUST-dg) and amphorized (Zn-HKUST-amorph) versions of each framework were studied by room temperature aqueous solution calorimetry. Comparing the energetics of both versions of the Cu and Zn frameworks provides insights into the thermodynamic role that a strongly coordinated solvent plays in the SBU and thus in overall framework stability.

MATERIALS AND METHODS

Cu-HKUST-H_2O. Cu-HKUST-1 was synthesized by combining $CuNO_3{\cdot}2.5H_2O$ and trimesic acid (TMA) in a 3:2 molar ratio and mixing into a 30 mL solution comprising equal parts of *N*,*N*-dimethylformamide (DMF), ethanol, and deionized water and heating at 85 °C for 20 h to yield small octahedral crystals. Phase purity of Cu-HKUST-H_2O was confirmed by powder X-ray diffraction (PXRD) (Figure S1). Thermogravimetric analysis (Figure S2) along with elemental analysis gave the formula $[Cu_3(TMA)_2{\cdot}3H_2O]{\cdot}5DMF$ (Table 1).

Zn-HKUST-DMF. Colorless cubes of Zn-HKUST-DMF were produced by reacting zinc nitrate and trimesic acid (TMA) in a 3:2 molar ratio in 30 mL DMF at 85 °C for 16 h; longer incubation times gave a product with poor crystallinity. This may be due to an increase of pH upon production of amine from the decomposition of DMF. Bulk sample purity was confirmed by PXRD (Figure S3). Previous investigations of Zn-HKUST-1 compared framework crystallinity against the simulated PXRD of Cu-HKUST-1. As this work sought to compare structural differences between the Cu and Zn SBUs, single crystal diffraction of Zn-HKUST-DMF was performed. Elemental analysis showed Zn-HKUST-DMF to contain 5 DMF molecules per formula unit, $[Zn_3TMA_2{\cdot}3DMF]{\cdot}2DMF$, i.e., 3 chemisorbed and 2 occluded DMF molecules (Table 1). The rapid collapse of Zn-HKUST-DMF to Zn-HKUST-amorph kinetically traps two additional DMF molecules inside the remaining structure, as revealed by elemental analysis. The remaining solvent is believed to be chemisorbed to the Zn atoms, giving the formula $[Zn_3TMA_2{\cdot}2DMF]$.

Cu-HKUST-dg. The activated framework (Cu-HKUST-dg) was made by exchanging with chloroform for 8 h eight times, followed by heating at 180 °C under vacuum overnight. Examination by PXRD after degassing confirmed crystallinity. The N_2 adsorption Brunauer–Emmett–Teller surface area is 1775.6 m^2/g (Figure S5). The Langmuir surface area is 1795.5 m^2/g. Both agree with literature findings,[24] confirming the evacuation of Cu-HKUST-dg. To compare the relative openness of Cu-HKUST-dg with other porous inorganic and hybrid frameworks, the molar volume (cm^3/mol) was calculated from the crystal structure to be 126.02 cm^3 per mole of Cu.

Zn-HKUST-amorph. Activation of Zn-HKUST-DMF was attempted by exchange with dry chloroform followed by evacuation at room temperature and at 180 °C overnight. PXRD of the chloroform exchanged Zn-HKUST-DMF framework showed that the framework retained its crystallinity. However after heating, the PXRD data of Zn-HKUST-amorph showed much lower crystallinity (Figure S6), suggesting partial framework collapse. Attempts to activate the sample under milder conditions, high vacuum at room temperature overnight, were also unsuccessful. These results mirror other reported attempts to activate Zn-HKUST-1.[25,26] Fourier transform infrared spectroscopy (FTIR), thermogravimetric analysis (TGA), and elemental analysis of the Zn-HKUST-amorph showed that some DMF remains despite prolonged heating under vacuum. Studies using positron annihilation lifetime spectroscopy[22,27,28] suggest the surface of the framework collapses partway into the activation process, thus trapping the remaining internal solvent as the outer pores collapse. To verify this, samples of Zn-HKUST-amorph were ground and analyzed by TGA. TGA of the ground Zn-HKUST-amorph sample showed the free release of DMF (Figure S7). Based upon elemental analysis, the final composition of Zn-HKUST-amorph is $Zn_3TMA_2{\cdot}2DMF$, although the final structure is unknown.

RESULTS AND DISCUSSION

The frameworks of Zn-HKUST-DMF, Zn-HKUST-chloroform and Zn-HKUST-amorph were examined by FTIR to identify changes in the Zn–O vibration, which in Zn-HKUST was centered at 455 cm^{-1} (Figure 2 and Figure S8). Little change in the Zn–O peak was seen after chloroform exchange. Upon thermal activation the Zn–O vibration split into three distinct peaks (450, 463, and 477 cm^{-1}), indicating a change in the initial symmetry likely due to deformation of the paddle wheel structure. This finding was also supported by Raman

dx.doi.org/10.1021/la4012839 | Langmuir 2013, 29, 8140–8145

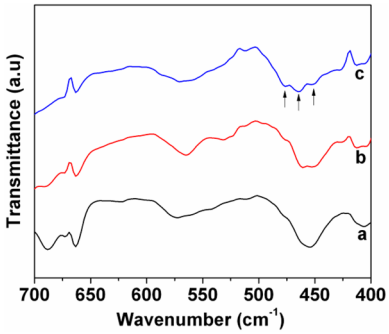

Figure 2. IR spectra of (a) Zn-HKUST-DMF, (b) Zn-HKUST-chloroform exchanged, and (c) Zn-HKUST-amorph at 180 °C for 12 h.

spectroscopy (Figure S9). The Zn-HKUST-DMF exhibited a vibrational mode at 160−190 cm^{-1}, which split into three broadened peaks at 212, 165, and 130 cm^{-1} in the Zn-HKUST-amorph sample. Characteristic peak splitting and peak broadening in the Zn-HKUST-amorph sample indicated deformation of the paddle wheel structure and loss of crystallinity.

The enthalpies of formation (ΔH_f) of the as-synthesized Cu-HKUST-H_2O and Zn-HKUST-DMF and the desolvated Cu-HKUST-dg and Zn-HKUST-amorph were measured by room temperature aqueous solution calorimetry,[29] utilizing a 2:1 (v/v) solution of 5 M hydrochloric acid and DMF. ΔH_f refers to formation of the framework and H_2O from dense assemblages (reaction 1 and 2): metal oxide (CuO or ZnO), H_3TMA, and in the as-synthesized structures DMF. Reported uncertainty is the standard error of the experimental average. To prevent rounding errors in further thermochemical calculations, two decimal places are given for all calorimetric measurements.

The ΔH_f of each framework was determined by applying the experimentally measured heats of solution (ΔH_s) of each component presented in either reaction 1 or 2 to the thermodynamic cycle (Table 2). Values for ΔH_s are found in Table 3. The obtained ΔH_f values (in kJ per mole of formula unit) are: Cu-HKUST-H_2O, −158.11 ± 0.95; Zn-HKUST-DMF, −162.66 ± 1.72; Cu-HKUST-dg, 49.97 ± 1.53 and Zn-HKUST-amorph, −10.71 ± 0.63. The ΔH_f (kJ per mole of metal) are: −52.70 ± 0.34 and −54.22 ± 0.57. The ΔH_f values for the activated Cu and Zn frameworks are: 16.66 ± 0.51 kJ per mole of Cu and −3.57 ± 0.21 kJ per mole of Zn. Per mole of metal, the solvent stabilization for Cu-HKUST-1 is −69.36 ± 0.19 kJ/mol, and the solvent contributes at least −50.65 ± 0.78 kJ/mol to the Zn- HKUST-1 stability. These values are similar to energetics seen in the interaction of water with metal oxide nanoparticles for which surface hydration enthalpies range from −60 to −120 kJ per mole of H_2O.[30,31] The strong stabilizing effect that DMF contributes to the Zn-HKUST-DMF framework suggests that the Zn paddle wheel SBU in the HKUST-1 framework is only stable in the presence of chemisorbed solvent. The removal of the DMF changes the coordination of Zn^{2+} from a five coordinate square pyramidal to square planar, a very unfavorable geometry for Zn. Previous thermochemical calculations of Zn^{2+} site preference in spinel solid solutions show Zn^{2+} to favor T_d coordination over O_h by −50 kJ/mol.[32] Though the Zn paddle wheel SBU is part of an open framework and not a spinel, a similarly strong thermodynamic preference for Zn^{2+} to T_d symmetry is likely a driver of Zn-HKUST-amorph structural collapse.

In the activation process all confined solvent, including the axial chemisorbed molecules, is removed. A recent density functional theory (DFT) study by Bureekaew et al.[38] of several coordination environments of Zn and Cu in paddle wheel SBUs showed the solvent-free Zn^{2+} paddle wheel SBU distorts to a D_{2d} symmetry, maximizing carboxylate oxygen distances.

The presence of orbital directing effects in the d^9 Cu^{2+} center leads to a preference for square planar coordination. The filled d^{10} orbitals of Zn^{2+} offer no coordination preference; thus the coordination geometry is driven solely by steric repulsion of the ligands. The computational study by Bureekaew and co-workers was performed with formate (a single carboxylate group COO^-) as the ligand, providing the simulated SBU a wide degree of freedom to optimize coordination geometry.[38] As the Zn SBUs in Zn-HKUST-amorph are interconnected by TMA, the collapse of the framework likely never reaches an optimum geometry, consistent with the PXRD showing a lack of long-range order (Figure S6). Notably, the simulation finds the loss of the first coordinated solvent molecule from the Zn SBU to induce a 53.1 kJ/mol increase in energy in the SBU, which is very similar to the 51.1 ± 0.8 kJ/mol endotherm observed by calorimetry. Though the solvent used in the computational study is pyridine which coordinates to Zn by nitrogen within the pyridine ring, while the DMF binds via the carbonyl oxygen, the magnitude of stabilization is strikingly similar.[38] Comparable results are seen theoretically for the removal of pyridine from the Cu SBU. DFT finds pyridine to stabilize the Cu SBU by −75.1 kJ per mole of Cu, while calorimetry shows the chemisorbed H_2O to be favorable by −69.4 ± 0.9 kJ per mole of Cu. Importantly, the large enthalpy difference between the Zn-HKUST-DMF and Zn-HKUST-amorph clearly illustrates the stabilization that the DMF solvent has upon the unfavorable coordination environment present in the Zn paddle wheel SBU.

The heat of solvation in Cu-HKUST-H_2O was found to be −69.4 ± 0.9 kJ/mol. This solvation enthalpy is the sum of both effects from chemisorbed and physisorbed solvent. However, the physisorbed guest is believed to contribute less than 5 kJ/mol based on previous calorimetric studies of solvent-MOF interactions.[14,15] Accounting for the physisorbed solvent, the Cu coordinated water is estimated to have a heat of adsorption of −65 ± 6 kJ per mole of Cu in the saturated system. Adsorption energies per H_2O for chemisorbed water in saturated systems have been calculated to be −47.3 kJ/mol and −52.8 kJ/mol by two separate studies.[39,40] The moderate difference between experiment and calculation suggests the need to refine models for solvent-metal coordination in MOFs, to that end new force fields are continuously being developed for metal−guest interactions.[41]

Providing accurate experimental heats of adsorption for the computation community is crucial to model development. The most common heat of adsorption cited in literature is the isosteric heat, which is the average heat of adsorption across the entire isotherm. For a material such as Cu-HKUST-1, which has two binding types (Cu-coordinated and physisorbed solvent), the isosteric heat of adsorption will produce an average of these two binding modes. Thus isosteric heats are likely to underestimate the heat of metal-solvent binding in systems with open metal sites. However experimental techniques to obtain energetics of gas adsorption at any point of an isotherm exist. Gas adsorption calorimetry developed by workers in the Peter A. Rock Thermochemistry Laboratory combines a Micromeretics ASAP 2020 gas analyzer with a Seteram Calvet microcalorimeter allowing controlled gas

dx.doi.org/10.1021/la4012839 | Langmuir 2013, 29, 8140−8145

Table 2. Thermodynamic Cycle Used To Calculate the Enthalpy of Formation of the M-HKUST-1 (M = Cu and Zn) System Measured in 2:1 (v/v) 5 M HCl and DMF

reaction scheme	enthalpy measurement[a]
$3M^{2+}(aq) + 2TMA^{3-}(aq) + x\ DMF(aq) + 3H_2O(aq) \rightarrow [M_3(TMA)_2(H_2O)_3]\ xDMF(cr)$	$\Delta H_1 = -\Delta H_s$(M-HKUST-1)[c]
$3 \times [MO(s) + 2H^+(aq) \rightarrow M^{2+}(aq) + H_2O(aq)]$	$\Delta H_2 = 3\Delta H_s$(MO)
$2 \times [H_3TMA\ (cr) \rightarrow TMA_{3-}(aq) + 3H^+(aq)]$	$\Delta H_3 = 2\Delta H_s$(H3TMA)
$x \times [DMF(l) \rightarrow DMF(aq)]$	$\Delta H_4 = x\Delta H_s$(DMF)[b]
$3 \times [H_2O(l) \rightarrow H_2O(aq)]$	$\Delta H_5 = 3\Delta H_{dil}(H_2O)$
$3MO(s) + {}_2H_3TMA(cr) + xDMF(l) \rightarrow [M_3(TMA)_2(H_2O)_3]\ xDMF(cr)$[c]	$\Delta H_f = \Delta H_1 + \Delta H_2 + \Delta H_3 + \Delta H_4 + \Delta H_5$

[a]All of the ΔH_s values can be found in Table 3. [b]x values for the as-synthesized frameworks can be found in Table 1. [c]For the thermodynamic cycle to calculate Zn-HKUST-DMF and Zn-HKUST-amorph, the coordinated H_2O shown above is replaced with the appropriate amount of DMF given in Table 1. The formation reactions (1 and 2) are:

$$3CuO(cr) + 2H_3TMA(cr) + xDMF(l) \rightarrow [Cu_3(TMA)_2 0.60x H_2O]xDMF(cr) + (3 - 0.60x)H_2O(l)$$

$$3ZnO(cr) + 2H_3TMA(cr) + xDMF(1) \rightarrow [Zn_3(TMA)_2(2 - x)DMF](3 - x)DMF(cr) + 3H_2O(l)$$

Table 3. Thermodynamic Data for Related Materials[a]

compound	ΔH_s kJ/(mol of formula)	ΔH_f kJ/(mol of formula)	ΔH_f kJ/(mol of T)	$\Delta H_{f,298K}$ kJ/(mol of formula)
CuO	−40.47 ± 0.06			−156.06 ± 2.09[b]
ZnO	−57.37 ± 0.01			−350.46 ± 0.27[c]
H_3TMA	17.28 ± 0.06			−1190.1 ± 0.9[d]
DMF	−9.45 ± 0.01			−239.4 ± 1.2[e]
H_2O	0.07[g]			−285.83 ± 0.04[f]
Cu-HKUST-H_2O	23.54 ± 1.06	−158.11 ± 0.95	−52.70 ± 0.34	−4203.49 ± 15.02
Cu-HKUST-dg	−137.31 ± 1.49	49.97 ± 1.53	16.66 ± 0.51	−1940.92 ± 6.42
Zn-HKUST-DMF	−21.95 ± 1.50	−162.66 ± 1.72	−54.22 ± 0.57	−3933.75 ± 10.21
Zn-HKUST-amorph	−128.25 ± 0.38	−10.71 ± 0.63	−3.57 ± 0.21	−3063.60 ± 5.52

[a]ΔH_s, enthalpy of solution at 2:1 (v/v) 5 N HCl and DMF at 298 K; ΔH_f, enthalpy of formation from components; $\Delta H_{f,298K}$, standard enthalpy of formation from elements. [b]Reference 33. [c]Reference 34. [d]Reference 35. [e]Reference 36. [f]Reference 37. [g]Small uncertainty excluded for convenience.

Table 4. Bond Lengths and Bond Angles of the Related Compounds to HKUST-1(Cu and Zn)

compound	M−M (Å)	M−O (Å) (oxide)	M−OOC (Å) (carboxylate)	M−O (Å) (solvent)	O−M−O (deg) (trans)	O−C−O (deg)
CuO[a]	2.900	1.956			180.00[e]	
ZnO[b]	3.209	1.978			110.85[f]	
Cu-HKUST-H_2O[c]	2.629		1.952	2.165	168.17	125.55
Zn-HKUST-DMF[d]	2.981		2.024	1.979	158.89	125.89

[a]Reference 43. [b]Reference 44. [c]Reference 20. [d]This work. [e]D_{4h} symmetry. [f]T_d symmetry.

dosing on a sample inside a calorimeter, allowing the direct measuring each gas dose.[30] This method provides a way to experimentally measure the heats of adsorption at each dose along the entire isotherm, including low pressure where the strongest binding occurs. Recently this method has been applied to MOFs, studying CO_2 heats of adsorption on CD-MOF-2 with excellent results, identifying three unique binding sites, two chemisorption sites, and one type of physisorption.[42]

The enthalpy of formation of the persistent Cu-HKUST-dg framework from its dense components is 16.66 ± 0.51 kJ/mol. This modest metastability and high molar volume (126.02 cm^3 per mole of Cu) for Cu-HKUST-dg is similar to values seen in previous thermodynamic studies of other MOFs and mesoporous inorganic materials.[12−15,38]

Traditional MOF analogies compare frameworks to a hub and spoke system, an illustration which captures the basic concepts of MOFs. Yet this model oversimplifies the complexities within the SBU system. While one can choose a linker with which to start, the SBU starting material is normally a metal salt. Choice of proper solvent in MOF syntheses likely affects reaction kinetics. However, in SBU systems with open coordination sites, like paddle wheel SBUs or high coordinate metal centers such as rare earth systems, chemically coordinated solvent may play a dominant thermodynamic role to stabilize the final structure.

The single crystal structure refinements (SI-2) offer further structural insights into the energetic differences. In the structures of as-synthesized Cu-HKUST-H_2O and Zn-HKUST-DMF, respectively, a single water or DMF molecule is bound axially to each metal center. The as-synthesized Cu and Zn frameworks are isostructural as illustrated by their identical centroid distances (Table S6). Though the as-synthesized Cu and Zn SBU have identical D_{4h} symmetries, each SBU has a slightly different bonding geometry (Table 4). The Cu−Cu distance is shorter (2.628 Å) than the Zn−Zn distance (2.981 Å). The trans O−M−O angles for the Cu and

dx.doi.org/10.1021/la4012839 | Langmuir 2013, 29, 8140−8145

Zn SBU are 168.17° and 158.89°, respectively, indicating the Cu SBU has a greater preference for a planar configuration of the carboxylate oxygens than the Zn SBU. The difference between the metal−solvent and metal−carboxylate distances in both SBUs parallels their relative stabilities. The structural preference of copper for the framework is clearly supported by the identical Cu−O bond lengths in Cu-carboxylate and CuO. Similarly, the zinc-solvent bond is similar to that in ZnO (Table 4). These structural characteristics parallel the thermochemical observations of each framework's stability.

CONCLUSION

The comparable energetics relative to a dense phase assemblage of the as-made Zn-HKUST-DMF and Cu-HKUST-H_2O document the major role of the solvent, with strong solvent-SBU interactions greatly stabilizing both frameworks. The framework of the otherwise unstable Zn-HKUST-1 can be obtained under the correct solvent conditions. This study may provide better understanding of the stability and structural insight of a porous framework based upon paddle wheel SBUs containing different transition metal ions. Energetics of the stable Cu-HKUST-dg follows trends seen in thermodynamic studies of other MOFs and ZIFs.

ASSOCIATED CONTENT

Supporting Information

Sample preparation, characterization, calorimetry, crystallographic information file, and crystallographic analysis. This material is available free of charge via the Internet at http://pubs.acs.org

AUTHOR INFORMATION

Corresponding Author

*E-mail: anavrotsky@ucdavis.edu.

Notes

The authors declare no competing financial interest.

ACKNOWLEDGMENTS

The authors thank the financial support of the Materials Science of Actinides, an Energy Frontier Research Center (EFRC) funded by the U.S. Department of Energy, Office of Science, Office of Basic Energy Sciences, under Award No. DE-SC0001089.

REFERENCES

(1) Furukawa, H.; Ko, N.; Go, Y. B.; Aratani, N.; Choi, S. B.; Choi, E.; Yazaydin, A.; Snurr, R. Q.; O'Keeffe, M.; Kim, J.; Yaghi, O. M. Ultrahigh Porosity in Metal-Organic Frameworks. *Science* **2010**, *329*, 424−428.

(2) Eddaoudi, M.; Kim, J.; Rosi, N.; Vodak, D.; Wachter, J.; O'Keeffe, M.; Yaghi, O. M. Systematic Design of Pore Size and Functionality in Isoreticular MOFs and Their Application in Methane Storage. *Science* **2002**, *295*, 469−472.

(3) Yoon, M.; Srirambalaji, R.; Kim, K. Homochiral Metal-Organic Frameworks for Asymmetric Heterogeneous Catalysis. *Chem. Rev.* **2012**, *112*, 1196−1231.

(4) Horcajada, P.; Gref, R.; Baati, T.; Allan, P. K.; Maurin, G.; Couvreur, P.; Férey, G.; Morris, R. E.; Serre, C. Metal-Organic Frameworks in Biomedicine. *Chem. Rev.* **2012**, *112*, 1232−1268.

(5) Corma, A.; García, H.; Llabrés i Xamena, F. X. Engineering Metal Organic Frameworks for Heterogeneous Catalysis. *Chem. Rev.* **2010**, *110*, 4606−4655.

(6) Dincă, M.; Dailly, A.; Liu, Y.; Brown, C. M.; Neumann, D. A.; Long, J. R. Hydrogen Storage in a Microporous Metal-Organic Framework with Exposed Mn^{2+} Coordination Sites. *J. Am. Chem. Soc.* **2006**, *128*, 16876−16883.

(7) Gadzikwa, T.; Farha, O. K.; Malliakas, C. D.; Kanatzidis, M. G.; Hupp, J. T.; Nguyen, S. T. Selective Bifunctional Modification of a Non-catenated Metal-Organic Framework Material via "Click" Chemistry. *J. Am. Chem. Soc.* **2009**, *131*, 13613−13615.

(8) Bétard, A.; Fischer, R. A. Metal-Organic Framework Thin Films: From Fundamentals to Applications. *Chem. Rev.* **2012**, *112*, 1055−1083.

(9) Wang, C.; Zhang, T.; Lin, W. Rational Synthesis of Noncentrosymmetric Metal-Organic Frameworks for Second-Order Nonlinear Optics. *Chem. Rev.* **2012**, *112*, 1084−1104.

(10) Cui, Y.; Yue, Y.; Qian, G.; Chen, B. Luminescent Functional Metal-Organic Frameworks. *Chem. Rev.* **2012**, *112*, 1126−1162.

(11) Sumida, K.; Horike, S.; Kaye, S. S.; Herm, Z. R.; Queen, W. L.; Brown, C. M.; Grandjean, F.; Long, G. J.; Dailly, A.; Long, J. R. Hydrogen Storage and Carbon Dioxide Capture in an Iron-Based Sodalite-Type Metal-Organic Framework (Fe-BTT) Discovered via High-Throughput Methods. *Chem. Sci.* **2010**, *1*, 184−191.

(12) Navrotsky, A.; Trofymluk, O.; Levchenko, A. A. Thermochemistry of Microporous and Mesoporous Materials. *Chem. Rev.* **2009**, *109*, 3885−3902.

(13) Navrotsky, A. Calorimetric Insights into the Synthesis of Templated Materials. *Curr. Opin. Colloid Interface Sci.* **2005**, *10*, 195−202.

(14) Hughes, J. T.; Navrotsky, A. MOF-5: Enthalpy of Formation and Energy Landscape of Porous Materials. *J. Am. Chem. Soc.* **2011**, *133*, 9184−9187.

(15) Hughes, J. T.; Bennett, T. D.; Cheetham, A. K.; Navrotsky, A. Thermochemistry of Zeolitic Imidazolate Frameworks of Varying Porosity. *J. Am. Chem. Soc.* **2013**, *135*, 598−601.

(16) Vagin, S. I.; Ott, A. K.; Rieger, B. Paddle-Wheel Zinc Carboxylate Clusters as Building Units for Metal-Organic Frameworks. *Chem. Ing. Tech.* **2007**, *79*, 767−780.

(17) Tan, K.; Nijem, N.; Canepa, P.; Gong, Q.; Li, J.; Thonhauser, T.; Chabal, Y. J. Stability and Hydrolyzation of Metal Organic Frameworks with Paddle-Wheel SBUs upon Hydration. *Chem. Mater.* **2012**, *24*, 3153−3167.

(18) Stylianou, K. C.; Rabone, J.; Chong, S. Y.; Heck, R.; Armstrong, J.; Wiper, P. V.; Jelfs, K. E.; Zlatogorsky, S.; Bacsa, J.; McLennan, A. G.; Ireland, C. P.; Khimyak, Y. Z.; Thomas, K. M.; Bradshaw, D.; Rosseinsky, M. J. Dimensionality Transformation through Paddle-wheel Reconfiguration in a Flexible and Porous Zn-Based Metal-Organic Framework. *J. Am. Chem. Soc.* **2012**, *134*, 20466−20478.

(19) Seo, J.; Bonneau, C.; Matsuda, R.; Takata, M.; Kitagawa, S. Soft Secondary Building Unit: Dynamic Bond Rearrangement on Multinuclear Core of Porous Coordination Polymers in Gas Media. *J. Am. Chem. Soc.* **2011**, *133*, 9005−9013.

(20) Chui, S. S. Y.; Lo, S. M. F.; Charmant, J. P. H.; Orpen, A. G.; Williams, I. D. A Chemically Functionalizable Nanoporous Material $[Cu_3(TMA)_2(H_2O)_3]n$. *Science* **1999**, *283*, 1148−1150.

(21) Wu, Y.; Qiu, L.-G.; Wang, W.; Li, Z.-Q.; Xu, T.; Wu, Z.-Y.; Jiang, X. Kinetics of Oxidation of Hydroquinone to p-Benzoquinone Catalyzed by Microporous Metal-Organic Frameworks M-3(BTC) (2) [M = Copper(II), Cobalt(II), or Nickel(II); BTC = Benzene-1,3,5-Tricarboxylate] using Molecular Oxygen. *Transition Met. Chem.* **2009**, *34*, 263−268.

(22) Feldblyum, J. I.; Liu, M.; Gidley, D. W.; Matzger, A. J. Reconciling the Discrepancies between Crystallographic Porosity and Guest Access As Exemplified by Zn-HKUST-1. *J. Am. Chem. Soc.* **2011**, *133*, 18257−18263.

(23) Kaye, S. S.; Dailly, A.; Yaghi, O. M.; Long, J. R. Impact of Preparation and Handling on the Hydrogen Storage Properties of Zn_4O(1,4-benzenedicarboxylate)$_3$ (MOF-5). *J. Am. Chem. Soc.* **2007**, *129*, 14176−14177.

(24) Rowsell, J. L. C.; Yaghi, O. M. Effects of Functionalization, Catenation, and Variation of the Metal Oxide and Organic Linking Units on the Low-Pressure Hydrogen Adsorption Properties of Metal-Organic Frameworks. *J. Am. Chem. Soc.* **2006**, *128*, 1304−1315.

(25) Ma, L. Q.; Jin, A.; Xie, Z. G.; Lin, W. B. Freeze Drying Significantly Increases Permanent Porosity and Hydrogen Uptake in 4,4-Connected Metal-Organic Frameworks. *Angew. Chem., Int. Ed.* **2009**, *48*, 9905−9908.
(26) Nelson, A. P.; Farha, O. K.; Mulfort, K. L.; Hupp, J. T. Supercritical Processing as a Route to High Internal Surface Areas and Permanent Microporosity in Metal-Organic Framework Materials. *J. Am. Chem. Soc.* **2009**, *131*, 458−460.
(27) Hibbe, F.; Chmelik, C.; Heinke, L.; Pramanik, S.; Li, J.; Ruthven, D. M.; Tzoulaki, D.; Kärger, J. The Nature of Surface Barriers on Nanoporous Solids Explored by Microimaging of Transient Guest Distributions. *J. Am. Chem. Soc.* **2011**, *133*, 2804−2807.
(28) Charlton, M.; Humberston, J. W. *Positron Physics*; Cambridge University Press: Cambridge, 2001.
(29) Hughes, J. T.; Navrotsky, A. Enthalpy of Formation of Zinc Acetate Dihydrate. *J. Chem. Thermodyn.* **2011**, *43*, 980−982.
(30) Ushakov, S. V.; Navrotsky, A. Direct Measurements of Water Adsorption Enthalpy on Hafnia and Zirconia. *Appl. Phys. Lett.* **2005**, *87*, 164103−164106.
(31) Navrotsky, A.; Ma, C.; Lilova, K.; Birkner, N. Nanophase Transition Metal Oxides Show Large Thermodynamically Driven Shifts in Oxidation-Reduction Equilibria. *Science* **2010**, *330*, 199−201.
(32) O'Neil, H. S. C.; Navrotsky, A. Cation Distributions and Thermodynamic Properties of Binary Spinel Solid-Solutions. *Am. Mineral.* **1984**, *69*, 733−753.
(33) Joint Army Navy Air Force; *JANAF Thermochemical Tables 2, Cr-Zr*; American Institute of Physics: New York, 1986.
(34) Cox, J. D.; Wagman, D. D.; Medvedev, V. A. *CODATA Key Values for Thermodynamics*; Hemisphere: New York, 1989.
(35) Yukhno, G. F.; Bikkulov, A. Z. Enthalpies of Combustion and Formation of Benzene Carboxylic Acids. *Russ. J. Phys. Chem. (Engl. Transl.)* **1971**, *45*, 924−925.
(36) Vasil'eva, T. F.; Zhil'tsova, E. N.; Vvedenskii, A. A. Enthalpies of Combustion of N,N-Dimethylformamide and N,N-Dimethylacetamide. *Russ. J. Phys. Chem. (Engl. Transl.)* **1972**, *46*, 315−318.
(37) Robie, R. A.; Hemingway, B. S. Thermodynamic Properties of Minerals and Related Substances at 298.15 K and 1 bar (105 pascals) Pressure and at Higher Temperatures. U.S. Geological Survey Bulletin No. 2131; U.S. Government Printing Office: Washington, DC, 1995.
(38) Bureekaew, S.; Amirjalayer, S.; Schmid, R. Orbital Directing Effects in Copper and Zinc Based Paddle-Wheel Metal Organic Frameworks: The Origin of Flexibility. *J. Mater. Chem.* **2012**, *22*, 10249−10254.
(39) Watanabe, T.; Sholl, D. S. Molecular Chemisorption on Open Metal Sites in Cu_3(benzenetricarboxylate)$_2$: A Spatially Periodic Density Fuctional Theory Study. *J. Chem. Phys.* **2010**, *133*, 094509.
(40) Grajciar, L.; Bludsky, O.; Nachtigall, P. Water Adsorption on Coordinatively Unsaturated Sites in CuBTC MOF. *J. Phys. Chem. Lett.* **2010**, *1*, 3354−3359.
(41) Zang, J.; Nair, S.; Sholl, D. S. Prediction of Water Adsorption in Copper-Based Metal-Organic Frameworks Using Force Fields Derived from Dispersion-Corrected DFT Calculations. *J. Phys. Chem. C* **2013**, *117*, 7519−7525.
(42) Wu, D.; Gassensmith, J. J.; Gouvêa, D.; Ushakov, S.; Stoddart, J. F.; Navrotsky, A. Direct Calorimetric Measurement of Enthalpy of Adsorption of Carbon Dioxide on CD-MOF-2, a Green Metal−Organic Framework. *J. Am. Chem. Soc.* **2013**, *135*, 6790−6793.
(43) Asbrink, S.; Norrby, L. J. A Refinement of Crystal Structure of Copper(2) Oxide with a Discussion of Some Exceptional ESDS. *Acta Crystallogr., Sect. B* **1970**, *26*, 8−15.
(44) Abrahams, S. C.; Bernstein, J. L. Remeasurement of Structure of Hexagonal ZnO. *Acta Crystallogr., Sect. B* **1969**, *25*, 1233−1236.
(45) Figures were constructed using VESTA a structural analysis program: Momma, K.; Izumi, F. VESTA 3 for Three-Dimensional Visualization of Crystal, Volumetric and Morphology Data. *J. Appl. Crystallogr.* **2011**, *44*, 1272−1276.